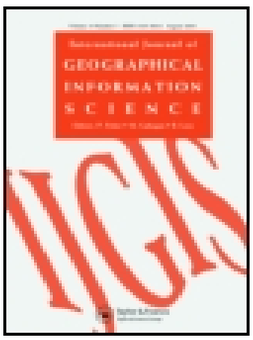

International Journal of Geographical Information Science

ISSN: 1365-8816 (Print) 1362-3087 (Online) Journal homepage: http://www.tandfonline.com/loi/tgis20

Historic reconstruction of reservoir topography using contour line interpolation and structure from motion photogrammetry

Ana Casado, Borbála Hortobagyi & Erwan Roussel

To cite this article: Ana Casado, Borbála Hortobagyi & Erwan Roussel (2018): Historic reconstruction of reservoir topography using contour line interpolation and structure from motion photogrammetry, International Journal of Geographical Information Science, DOI: 10.1080/13658816.2018.1511795

To link to this article: https://doi.org/10.1080/13658816.2018.1511795

Published online: 05 Sep 2018.

INTERNATIONAL JOURNAL OF GEOGRAPHICAL INFORMATION SCIENCE
https://doi.org/10.1080/13658816.2018.1511795

Taylor & Francis
Taylor & Francis Group

RESEARCH ARTICLE

Historic reconstruction of reservoir topography using contour line interpolation and structure from motion photogrammetry

Ana Casado [a,b], Borbála Hortobagyi[b,c] and Erwan Roussel[b]

[a]Departamento de Geografía y Turismo, Universidad nacional del Sur, Bahía Blanca, Argentina; [b]Université Clermont Auvergne, CNRS, GEOLAB, F-63000, Clermont-Ferrand, France; [c]School of Geography, Politics and Sociology, Newcastle University, Newcastle upon Tyne, UK

ABSTRACT

The geometry of impounded surfaces is a key tool to reservoir storage management and projection. Yet topographic data and bathymetric surveys of average-aged reservoirs may be absent for many regions worldwide. This paper examines the potential of contour line interpolation (TOPO) and Structure from Motion (SfM) photogrammetry to reconstruct the topography of existing reservoirs prior to dam closure. The study centres on the Paso de las Piedras reservoir, Argentina, and assesses the accuracy and reliability of TOPO- and SfM- derived digital elevation models (DEMs) using different grid resolutions. All DEMs were of acceptable quality. However, different interpolation techniques produced different types of error, which increased (or decreased) with increasing (or decreasing) grid resolution as a function of their nature, and relative to the terrain complexity. In terms of DEM reliability to reproduce area–elevation relationships, processing-related disagreements between DEMs were markedly influenced by topography. Even though they produce intrinsic errors, it is concluded that both TOPO and SfM techniques hold great potential to reconstruct the bathymetry of existing reservoirs. For areas exhibiting similar terrain complexity, the implementation of one or another technique will depend ultimately on the need for preserving accurate elevation (TOPO) or topographic detail (SfM).

ARTICLE HISTORY
Received 20 April 2018
Accepted 9 August 2018

KEYWORDS
Contour line interpolation; structure from motion photogrammetry; DEM accuracy; DEM reliability; Paso de las Piedras reservoir

Introduction

World's rivers are impounded by more than 45,000 large dams, from which about 60% operate primarily or exclusively for irrigation and water supply (WCD 2000). Although many dams were built recently – or are currently under construction –, the average large dam today is about 50 years old. Aged dams providing water from reservoirs face a number of problems. From these, two major concerns are (i) the increased demand for water, owing to population growth and increased consumption per capita, and (ii) the gradual loss of the reservoir storage capacity by sedimentation, all of which prevents the supplying service for which the dam was designed and reduces its operating life (Annandale 2013, Kondolf *et al.* 2014). Furthermore, increasing concern on the impacts of climate change has motivated

CONTACT Ana Casado ana.casado@uns.edu.ar

substantive (re)evaluations of the ability of completed dams to yield water at some level of reliability, including assessment and projections of reservoir storage capacities (Kang *et al*. 2007, Kim *et al*. 2009, Watts *et al*. 2011, Ceylan and Ekizoglu 2014, Soundharajan *et al*. 2016, Ehsani *et al*. 2017, Ho *et al*. 2017). Aside from the evaluation of changes in water inflows and outflows, assessment and projection of reservoir storage capacities involve an accurate appreciation of the impounded geometry. This is achieved based on historic topographic data, bathymetric surveys, remote sensing data, and sedimentation models. Indeed, the so-called area-volume-elevation curve (AVE) is a key tool to manage the reservoir storage capacity (Cross and Moore 2014, Sayl *et al*. 2017).

One major concern is that detailed topographic data prior to dam closure are unavailable for many projects, and bathymetric surveys allowing reconstructing rates of reservoir sedimentation may be absent or discontinuous in space and time. Therefore, rates of capacity loss remain unknown – or need to be updated – for many reservoirs worldwide. In the absence of historic topographic and bathymetric surveys, the surface impounded by average-aged reservoirs may be reconstructed using two historical sources of elevation data: (i) contours extracted from topographic maps, and (ii) historical aerial photographs. Both data sources are widely available and provide detailed information on terrain elevation and forms. Yet the process for extracting and processing elevation data from these sources presents a number of pros and cons. Contour- and photogrammetry-derived digital elevation models (DEMs) are standard tools in geosciences, and their applicability to Earth surface and environmental analyses has been tested and proved by countless studies. However, the quality of contour-derived DEMs is markedly affected by the processing technique (interpolation and sampling) relative to the density of contours and the configuration of the terrain surface (Wise 2000, Hengl *et al*. 2004, Fisher and Tate 2006). On the other hand, photogrammetric techniques are frequently time-consuming, necessitate a more expensive equipment, and require specialized user expertise. In recent years, the Structure from Motion (SfM) has developed into a fast, low-cost and user-friendly tool to obtain three-dimensional data (dense point clouds) of a scene from a series of unordered overlapping images and ground control points (Westoby *et al*. 2012, Fonstad *et al*. 2013, Micheletti *et al*. 2015a, Carrivick *et al*. 2016). SfM has known an expansion in various fields because of its greater ease of use where expert supervision is unnecessary (Micheletti *et al*. 2015b). However, the focus of most SfM applications has been the collection and analysis of new photography (Warrick *et al*. 2017). Recent studies have tested the compatibility of SfM with pre-existing aerial photography to detect changes in volcano landscapes (Derrien *et al*. 2015, Gomez *et al*. 2015), in coastal landscapes (Warrick *et al*. 2017), and in glacier landscapes (Mertes *et al*. 2017, Mölg and Bolch 2017). They found that historical photographs might fulfil quality and overlap requirements, which implies a great expansion of SfM applications.

This paper examines and compares the potential of traditional contour line interpolation and new SfM photogrammetry to reconstruct the topography beneath aged reservoirs using two affordable and widely available sources of elevation data. It seeks to address two major questions: (1) how accurate and reliable are the DEMs obtained from historical sources of elevation data given their inherent quality issues; and (ii) for similar processing-related time cost and expertise, what is the processing technique that best fit to reconstruct the bathymetry of average-aged reservoirs in regions where

topographic surveys prior to impoundment are unavailable or unreliable. In addition to providing a new example of the application of SfM photogrammetry using historic aerial photography, this study implements a robust methodology allowing determining the quality of DEMs reproducing past topography. The DEMs produced herein have direct applicability as a proxy of historical bathymetric data. Bathymetric reconstructions of aged reservoirs underpin further development of sedimentation models and hydrological derivatives, and therefore have great potential for applicability as a water management tool.

Materials and methods

Study site

The study centres on the reservoir Paso de las Piedras on the Sauce Grande River, a middle-size basin excavated within a dry sub-humid, sub-mountain plain located in south-western Buenos Aires, Argentina (Figure 1). Mean annual rainfall decreases from 800 mm in the uplands to 640 mm in the lowlands, and elevation ranges from 1240 m in the headwaters (Ventania Range) to 60 m on the frontal scarp that separates the plain from the coastal zone. Dominant land uses are rain-fed agriculture and livestock grazing of unimproved grasslands; population density within the river basin is very low. The reservoir operates since 1978 for drinking water supply to a population that today exceeds 350,000 people and concentrates in the cities of Bahía Blanca and Punta Alta.

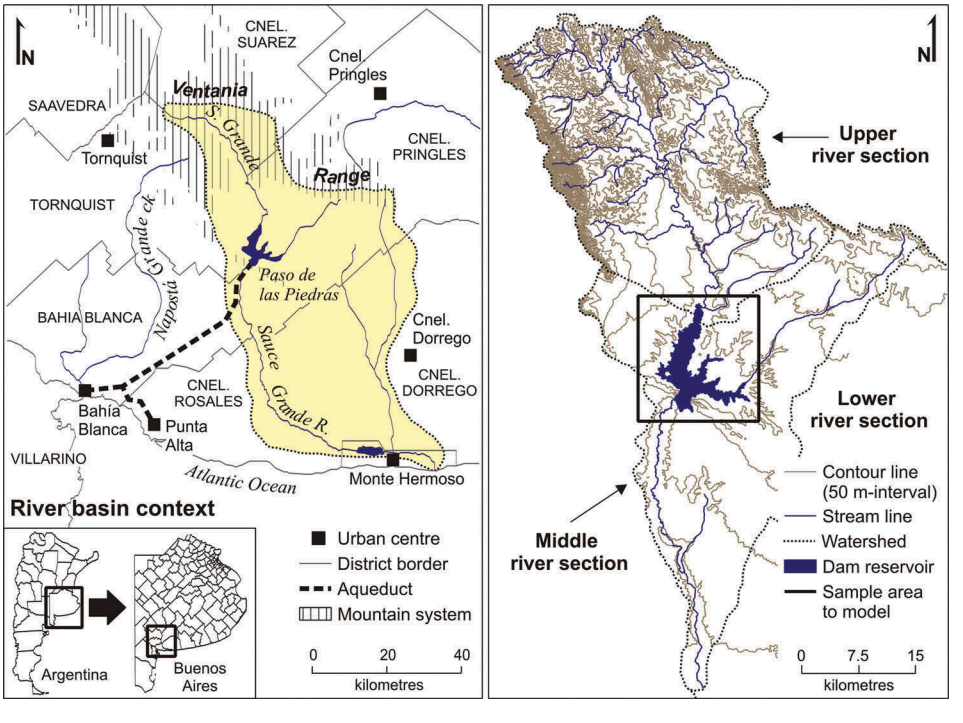

Figure 1. Map of the study area showing the regional context of the reservoir Paso de las Piedras (Argentina) and the DEM sampling area.

At full supply, it has a surface area of 36 km^2, depth of 25 m, and maximum capacity of 328 $m^3 10^{-6}$ (Schefer 2004). The river flow regime is rain-fed and flashy; mean annual flow is 4.54 $m^3\ s^{-1}$, and peak flows may reach more than 1000 $m^3\ s^{-1}$ in few hours. Inter-annual flow variability is marked, and linked primarily to alternating phases of El Niño – Southern Oscillation phenomenon (Scian 2000) inducing episodes of drier- and wetter-than-normal climate (Campo *et al*. 2009, Bohn *et al*. 2011). Increasing water demand due to population growth and decreasing water availability due to recurrence of drought combine to generate low resilience to water scarcity, and impact very seriously on the efficiency and sustainability of local water resources management.

DEM processing

We have produced eight DEMs using a combination of (i) two processing techniques, contour line interpolation and SfM photogrammetry, and (ii) four different output resolutions (5, 10, 30, and 50 m). The models were produced for a sample area of 455 km^2 delimited within the middle river basin (Figure 1). In addition to containing the topographic depression impounded by the reservoir, this area is particularly interesting because it includes a combination of ridges, plains and valleys providing a variety of landforms on which to test the accuracy and the reliability of the DEMs. Elevation within the sample area ranges from 295 m on the top ridge to 128 m on the valley bottom. Note that the area used to extract the models was reduced by 2.5-km side to avoid boundary distortions during model processing. All models were projected using UTM coordinates to ensure compatibility between different sources of information; elevation values, however, refer to the Campo Inchauspe datum as it constitutes the reference system used in Argentina until the 90's.

Topographic data extraction

The sample area is located at the intersection of four contiguous topographic map sheets (1:50,000) produced between 1962 and 1968 by the Instituto Geográfico Militar, now Instituto Geográfico Nacional (IGN, Argentina). Scanned versions of the maps (600 dpi) were corrected by polynomial restitution using the intersections of the projection grid (Gauss-Krüger). From these, we have extracted four sets of topographic data (Figure 2). These included (i) 10-m interval contour lines, (ii) streamlines, (iii) spot elevations in visible ground locations such as road junctions and parcel plots (calibration points), and (iv) spot elevations in less visible ground locations such as topographic and geodesic benchmarks (validation points). It should be noted that both contour- and SfM-derived DEMs were produced using the same set of calibration points to ensure coherence of the results.

Contour-derived DEMs

The models were created using the Topo to Raster command in ArcGIS (TOPO), a thin plate spline method based on the algorithm developed by Hutchinson (1988, 1989)). Interpolation used contours as primary type of elevation data, calibration points, and streamlines (Figure 2). In addition to working intelligently with contour data (primary type of input data), TOPO infers flow paths and removes false sinks to produce a hydrologically correct raster surface. TOPO does not require prior transformation of the input data, yet one

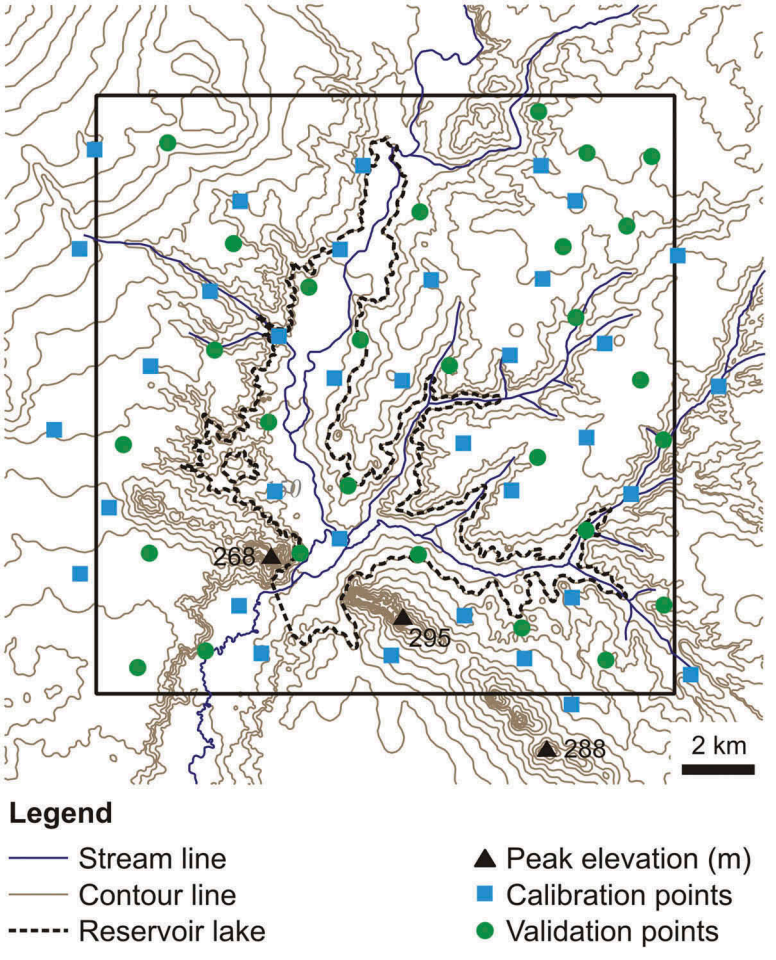

Figure 2. Topographic data used to generate the DEMs and to validate their vertical accuracy. The DEM sampling area is illustrated using a thick black line.

must ensure that streamline arcs point in the downstream direction and that contour lines for equal elevation levels are merged correctly.

SfM-derived DEMs

SfM is a new photogrammetric technique for surface restitution relying on the most recent automated image matching approach (Fonstad *et al*. 2013, Warrick *et al*. 2017). This study uses SfM to (i) produce dense clouds of topographic points from sequences of historic aerial photography, and (ii) create a DEM from interpolation of the dense point cloud. SfM analysis was conducted entirely in Agisoft PhotoScan Pro (v.1.2.5). Inputs included 31 scanned aerial photographs (1200 dpi) dating from 1961 (1:35,000; IGN). Photo quality index ranges between 0.81 and 0.94, photo end lap is ~ 60%, and photo side lap is ~ 30%. By default, PhotoScan estimates intrinsic camera parameters for photo alignment based on the information contained in EXIF meta-data. In the absence of EXIF files, camera groups were calibrated manually by fixing the focal length (shown in the inscription of the photographs) and the pixel size (calculated as the quotient between

the number of pixels and the image size). Other pre-processing steps included (i) setting the camera precision according to the measurement accuracy of old photographs, and (ii) masking the lateral inscriptions of the photographs and boundaries exhibiting a high degree of distortion.

DEM extraction followed the standard SfM workflow, namely (i) photo alignment, (ii) 3D point cloud extraction, and (iii) DEM generation (Westoby *et al*. 2012, Fonstad *et al*. 2013). As camera positions were unknown, photo alignment used high accuracy and generic pair preselection settings. It also constrained features by mask to avoid including photo boundaries and lateral inscriptions in the alignment process. Initial camera positions were optimized using a set of 35 Ground Control Points (GCP) corresponding to the set of calibration points extracted from the topographic maps (Figure 2). Unlike conventional photogrammetry, SfM requires a small number of GCP to scale and reference point clouds (Fonstad *et al*. 2013, Micheletti *et al*. 2015b). The 3D point cloud was extracted from optimized camera positions using aggressive depth filter to remove small surface details. In the second step, results were classified to differentiate ground points from noise and unclassified elements of the terrain surface such as vegetation and buildings. The DEM was generated using the cloud of ground points only. This last step permitted to eliminate some errors of the model automatically. The models were then exported into .tiff format to be incorporated in ArcGIS.

DEM quality assessment

One of the greatest challenges to assess the quality of DEMs that reconstruct past topography is the overall lack of historic elevation data on which to base descriptive statistics of error. In areas impounded by average-aged reservoirs, such as it is the focus of this study, this challenge is even greater because the terrain surface has been progressively covered by water. Since the elevation parameters of both TOPO and SfM models build on the pre-existing cartography, it follows that elevation values obtained from the topographic maps provide the most reasonable basis on which to test the vertical accuracy of the models. However, this procedure provides a simple, global summary of error, and may not assist in identifying the source of error (Wise 2000). As reported by Fisher and Tate (2006), elevation-based DEM quality assessments may fail to describe the spatial pattern of error, and in a DEM errors are likely to vary spatially. This study implements an integrative DEM quality assessment that considers (i) the DEM accuracy to reproduce actual terrain elevation and shapes, and (ii) the DEM reliability to preserve spatial patterns of topography (Figure 3). Whereas accuracy measures the fit between de DEM and the terrain surface, reliability measures the quality of DEM-derived products (Desmet 1997, Wise 2000, Hengl *et al*. 2004), namely area–elevation relationships for the purpose of this paper.

Accuracy assessment

The first step in assessing the DEM accuracy consisted in determining the fit between a sample of elevation points extracted from the models (Z_{DEM}) and known elevations extracted from the topographic maps (Z_{REF}). Errors were reported as the mean error (ME) and the root mean square error (RMSE), both metrics being popularly used as an indicator of bias and statistical distribution of error, respectively (Fisher and Tate 2006). A more

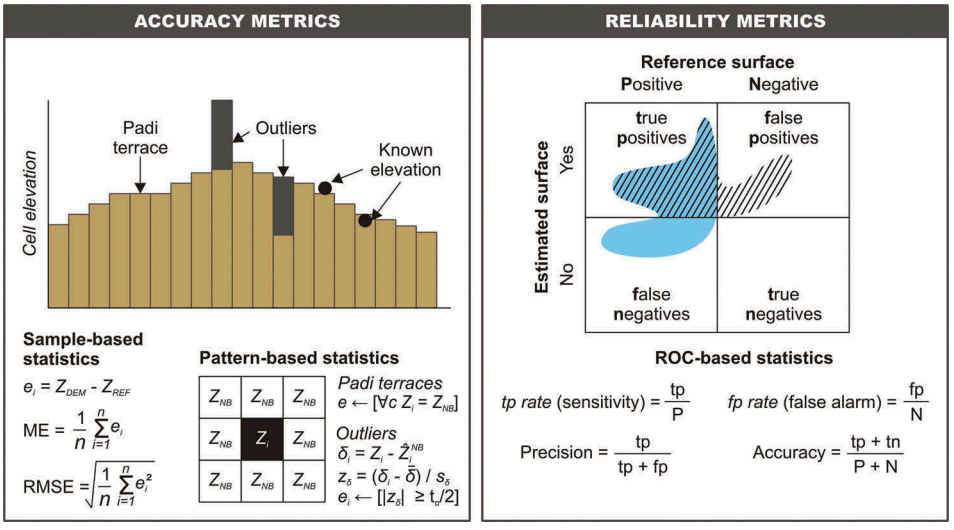

Figure 3. Accuracy and reliability metrics used in DEM quality assessment. Left: modified from Hengl *et al*. (2004); right: modified from Fawcett (2006).

comprehensive approach, however, consists in determining DEM errors based on patterns of values rather than on isolated samples (Wise 2000). These errors are commonly referred to as relative errors, and may be detected using neighbourhood analysis in a Geographic Information System (GIS). According to Hengl *et al*. (2004) two common types of relative error are (i) padi terraces or cut-offs, defined as artificial flat areas where all cells have the same elevation value; and (ii) outliers, defined as isolated cells with anomalous, improbable elevation values.

Padi terraces were detected using metrics of variety, which computes the number of unique cell values within focal neighbouring windows (Figure 3). For a 3 × 3 neighbouring window variety ranges from 1 to 9, where 1 indicates that all nine cells have the same elevation value and 9 indicates the opposite. The algorithm requires integer values as input, so that DEMs were multiplied by 100 to preserve 1 cm-precision in cell elevation values. *Outliers* were detected using the statistical approach of Felicísimo (1994), which builds on probability distributions of error across the entire DEM. Errors were calculated on a cell-by-cell basis by comparing the original elevation value of a DEM (Z_i) with the elevation value estimated from its neighbours ($\hat{Z}_i^{NB}$). Given the assumption of smooth terrain, differences between Z_i and $\hat{Z}_i^{NB}$ should be small (Wise 2000). Outliers are therefore detected from extreme deviations of normalized residuals using a simple Student's *t* test (Figure 3). For the two-tail 99.9% probability ($\alpha = 0.001$) the value of *t* is 3.291.

Absolute and relative accuracy metrics were computed globally as well as separately for areas exhibiting different degree of terrain slope. This provided an idea of the spatial distribution of errors across the models. Slope classes include flatlands (<0.5°), lands gently inclined (0.5° to 2°), and rolling lands (>2°).

Reliability assessment

The DEM ability to reproduce area–elevation relationships for varying reservoir water levels (or reservoir depths) was inspected using the Receiver Operating Characteristics

(ROC) approach (Figure 3). Reference surfaces were obtained from classification of 17 Landsat images (30 m-resolution) capturing the reservoir lake for varying water levels ranging from low (143 m a.s.l.; 3 m-depth) to high (165 m a.s.l.; 25 m-depth). The vertical spacing between consecutive reference surfaces is ± 1 m, except for reference surfaces between 145 and 154 m a.s.l. where the vertical spacing is ± 3 m. Image classification was achieved in ArcGIS using near-infrared (NIR) and shortwave infrared (SWIR) bands to clearly differentiate the waterbody delineated by the reservoir lake (Frazier and Page 2000). Corresponding surface estimates were obtained from reclassification of the DEMs into two classes delimited by the absolute water levels identified above. This produced 17 maps by primary model type and sampling resolution (i.e. 136 maps in total) reproducing the surface that would be impounded for a given reservoir water level (or reservoir depth).

Confusion matrices classified the DEM-derived surface for a given water level (estimated impounded surface) against the reference surface extracted from satellite imagery (real impounded surface). This provided four classes of outcomes by reservoir water level: (i) impounded surfaces classed as impounded surfaces counted as *true positives*; (ii) impounded surfaces classed as not impounded surfaces counted as *false negatives*; (iii) not impounded surfaces classed as not impounded surfaces counted as *true negatives*; and (iv) not impounded surfaces classed as impounded surfaces counted as *false positives*. This matrix constitutes the basis for a number of common metrics of model performance, namely, sensitivity (or recall), false alarm, precision and accuracy (Fawcett 2006). ROC curves usually compare true positive rates (i.e. proportion of positives correctly classified relative to the total positives) and false positive rates (i.e. proportion of negatives incorrectly classified relative to the total negatives) to illustrate trade-offs between model sensitivity (or recall) and false alarm (Fawcett 2006). This study uses the metric of precision (i.e. proportion of true positives relative to the sum of false positives and true positives) instead of the false positive rate because in spatial analysis the total number of negatives may be as large as the area delimited for analysis. As argued by Saito and Rehmsmeier (2015), precision-recall curves (PRC) perform better when evaluating binary classifiers on imbalanced datasets, such as it is the case in spatial analysis.

Results

DEM accuracy

Coefficients of determination between elevation estimates and known elevations extracted from the topographic maps (validation points) were close to unity for all eight DEMs suggesting well-fitted models (Figure 4). The ME was between −0.3 and −0.4 m for TOPO models, and between 1.7 and 1.8 m for SfM models; the error dispersion (RMSE) ranged from 2.2 to 3.3 m, and from 5.3 to 6 m, respectively. Interestingly, minimum absolute errors increased in magnitude with increasing grid cell size for both model types. This indicates a tendency to lowering elevation with increasing terrain smoothing, the coarser DEMs (50 m-resolution) showing the greatest RMSE. Another interesting aspect is that the ME was negative for all models. Although small ME values indicate that positive and negative bias are uniformly distributed, the

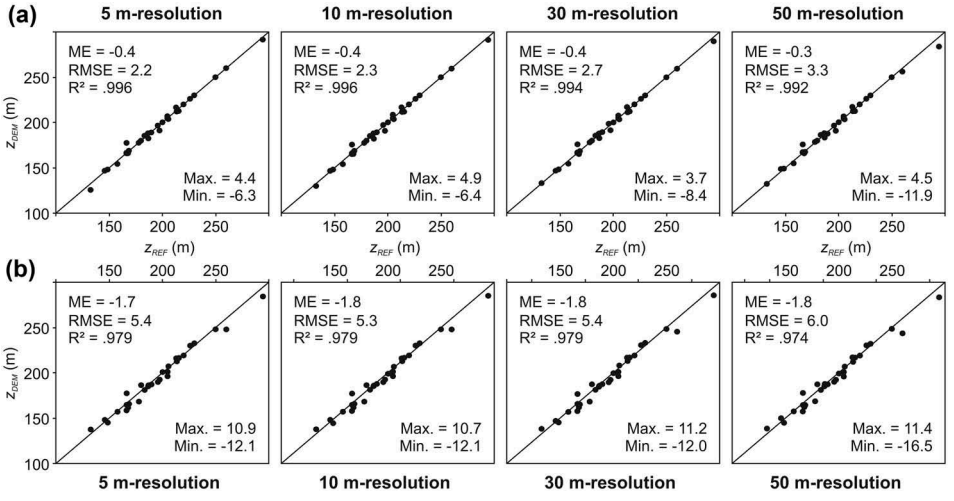

Figure 4. Vertical accuracy of [A] TOPO models and [B] SfM models by sampling resolution. The coefficient of determination (R^2) from model predictions and error statistics are given along.

negative sign indicates an overall tendency to underestimation of elevation irrespective of the processing technique and the sampling resolution of the DEMs.

Figure 5 illustrates the distribution of elevation errors as a function of varying terrain slope. Errors from TOPO interpolation were more pronounced in flatlands (class 1) and in rolling lands (class 3) than in lands gently inclined (class 2), and increased with increasing grid cell size at rates of between 3 and 7% (class 1) and between 3 and 60% (class 3).

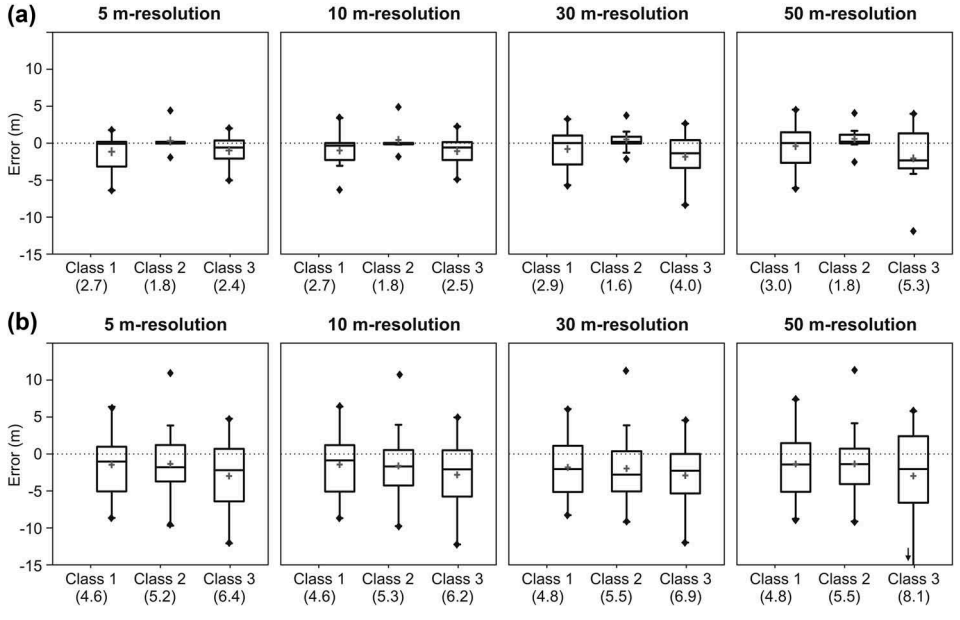

Figure 5. Distribution of elevation errors from [A] TOPO models and [B] SfM models by sampling resolution and terrain slope class. The RMSE by slope class is shown in parenthesis.

This indicates a complex relationship between contour density, grid resolution and terrain complexity. Errors in flatlands result from inadequate contour density to derive an accurate interpolation of the terrain surface in areas of low relief, and increase gradually with increasing grid cell size as a consequence of terrain smoothing. As the terrain slope increases, the density of contours increases as well and the vertical model accuracy improves. Yet the RMSE in rolling lands remains higher than the RMSE in lands gently inclined. This occurs because, in areas of high relief, such as hills and ridges, extrapolation from closed contours or scale-dependent suppression of contours may result in large elevation errors. A second aspect to highlight is the inadequacy of the coarsest TOPO models to reproduce the complexity of the terrain surface. Relative to 10 m-TOPO, the RMSE from 30 m-TOPO increments by 7% (class 1) and by 60% (class 3), and the RSME from 50 m-TOPO increments by 11% and by 112%, respectively. In opposition, errors from SfM restitution were notably more affected by terrain slope than by varying grid cell size. The RMSE increased with increasing terrain inclination up to 15% between class 1 and 2, and up to 54% between class 2 and 3. An interesting aspect is that elevation errors were relatively fairly distributed for all terrain classes and model resolutions, and exhibited an overall tendency to underestimation of altitude that was notably most marked in areas of steep terrain. These aspects indicate deficiencies in DEM processing relative to the quality and texture of the photographs, the accuracy in the identification of ground control points, or both.

Contrasting results emerged from pattern-based error assessment. SfM models exhibited the greatest variety in neighbouring elevation values for all sampling resolutions (Figure 6 (a)), with differences of up to + 15% relative to TOPO models of equal resolution. Variety distributions with varying terrain slope differentiated SfM from TOPO models as well (Figure 6 (b)). Whereas SfM models exhibited similar variety distributions for all three terrain slope classes, TOPO models showed clear concentration of low variety values in flatlands (e.g. variety is less than 4 for 29% of cells in 5 m-TOPO) and high variety values in rolling lands (e.g. variety is more than 6 for 57% of cells in 5 m-TOPO). Despite these variety differences between primary model types, the proportion of paddy terraces (i.e. cells showing equal elevation values) decreased with increasing grid cell size for both SfM and TOPO models. Naturally, padi terraces are increasingly removed with decreasing resolution because elevation values result progressively from interpolation of greater neighbouring elevation areas.

On the other hand, outlier assessment revealed that both TOPO and SfM models perform fine. Percent of outliers (i.e. proportion of anomalous cell values relative to the total number of cells) was near 1% for all eight DEMs (Figure 7), although TOPO models exhibited smallest error ranges than SfM models (−0.9 m to 4.9 m and −28.1 m to 11.7 m, respectively). Interestingly, outliers in TOPO models increased in proportion and magnitude with increasing grid cell size, whereas outliers in SfM models decreased in proportion but increased in magnitude. This is closely related to the way errors distribute across the models, relative to the configuration of the terrain surface and to the method used to detect them. Outliers in SfM models distribute randomly on the terrain surface reflecting texture changes between overlapping images, and tend to cluster in noisy areas were reflectance is affected by topographic effects (e.g. 45 to 53% of outliers are localised in rolling lands). Isolated anomalous cell values are increasingly removed with increasing grid cell size as a consequence of terrain smoothing. Outliers clustered in

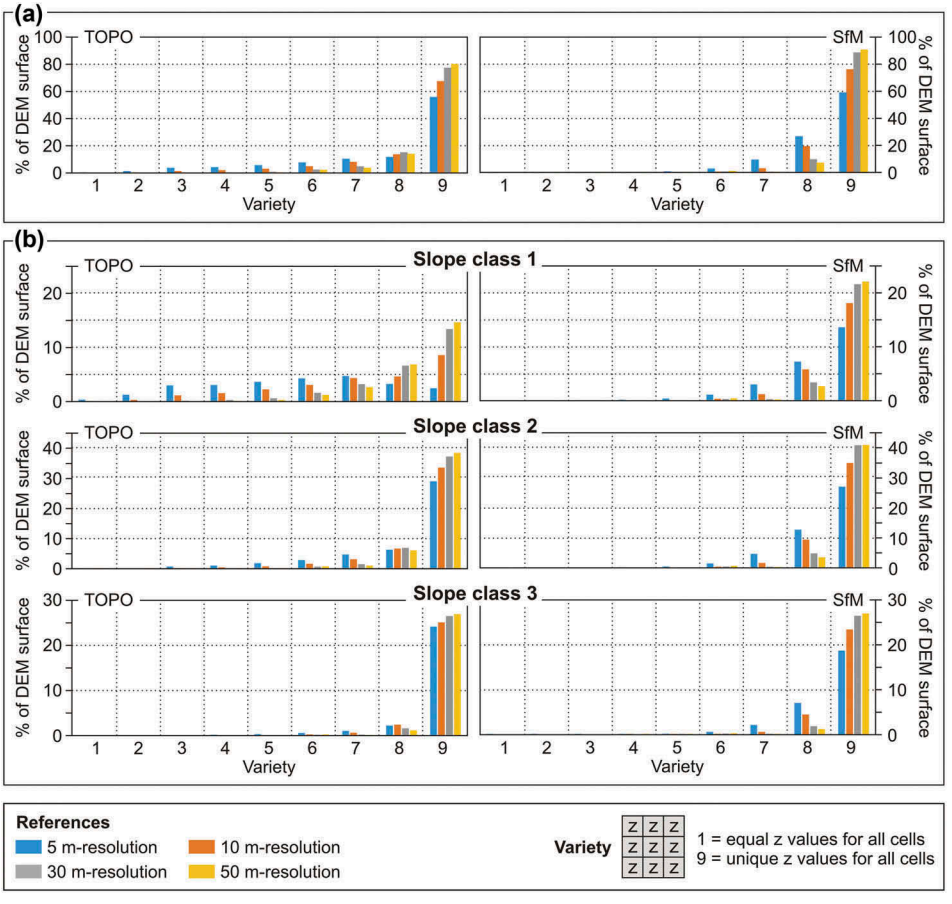

Figure 6. Elevation variety by primary DEM type and sampling resolution (a) and variety distributions by terrain slope class (b).

steep areas, however, are not necessarily removed with increasing grid cell size but increased in magnitude because the difference between original elevation values and elevation values estimated from the neighbouring cells also increases. This tendency is also found in TOPO models, where outliers are markedly clustered in rolling lands and increase in proportion with grid cell size from 83 to 87%. In these cases, outliers may not necessarily indicate a source of error but the inability of low-resolution models to reproduce elevation in areas of steep terrain accurately.

DEM reliability

Irrespective of accuracy-related disagreements, both TOPO and SfM models are highly reliable to reproduce impounded surface areas for varying reservoir water levels (Figure 8). Linear correlations are close to unity in all cases, although residuals occur and are most marked in the lowest extreme of the distribution. This indicates a better model adjustment to simulate area–elevation relationships at high reservoir levels, but a model inability to reconstruct such relationships with

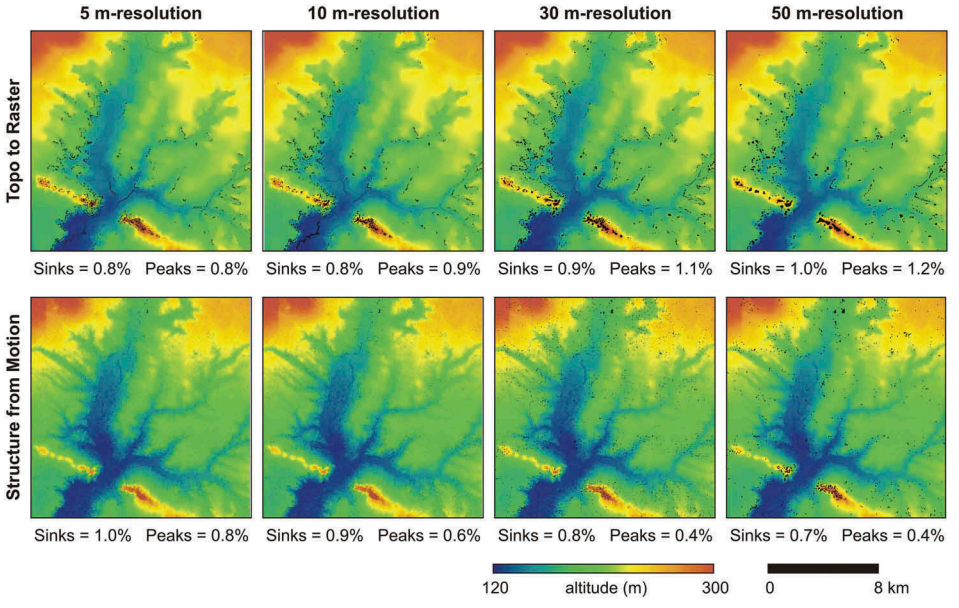

Figure 7. Probability maps showing the spatial distribution of outliers (black surfaces) by primary DEM type and sampling resolution. Corresponding original DEMs are used to illustrate the configuration of the terrain surface.

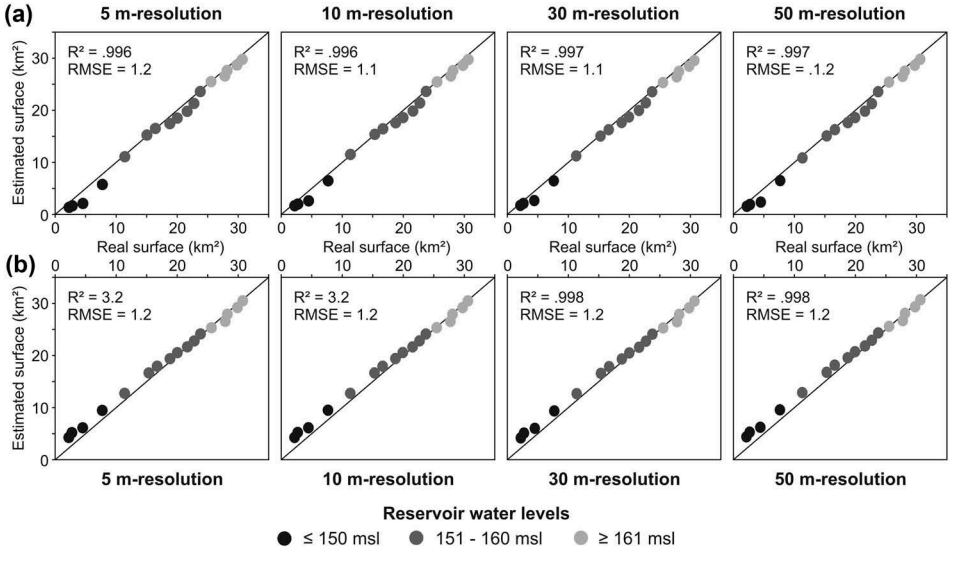

Figure 8. Scatterplots comparing impounded surface areas for varying reservoir levels and corresponding surfaces estimated from (a) TOPO models and (b) SfM models by sampling resolution. The coefficient of determination (R^2) and the RMSE from model predictions are given along.

increasing reservoir depth. Since the vertical spacing between consecutive area-elevation reference maps for the lowest reservoir water levels is ± 3 m, it follows that vertical errors may attain as much as ± 3 m depth. In terms of surface area, expressed as the proportion of the real surface area impounded for a given

elevation level, residuals were up to + 93% (SfM; 143 m a.s.l.) and −43% (TOPO; 145 m a.s.l.). The influence of varying topography on the reliability of TOPO- and SfM-derived DEMs was notably more important than the influence of varying DEM resolution.

This latter aspect is clearly reflected by PRC curves (Figure 9). Classifiers appearing in the upper right corner (1, 1) represent the best compromise between the model sensitivity to estimate the surface impounded for a given reservoir water level and the model precision to avoid classification of surfaces that are not really impounded for that reservoir water level. Such classifiers correspond to maps reproducing impounded surfaces for medium to high reservoir water levels (≥ 151 m a.s.l.). As the vertical spacing between these maps is ± 1 m, it follows that TOPO and SfM models are not only performing to reproduce area–elevation relationships within the topographic depression that contains the reservoir lake but also to maintain such relationships within a range of vertical error smaller than 1 m-depth. As for the lowest reservoir water levels (i.e. water levels near the maximum reservoir depth), PRC curves separate TOPO and SfM models into two well-defined, contrasting groups. TOPO models produce the lowest true positive rates ($0.44 < tp < 0.76$) with the highest precision rates ($0.84 < p < 0.92$), whereas SfM models produce the highest true positives rates ($0.81 < tp < 0.95$) with the lowest precision rates ($0.42 < p < 0.77$). This indicates that TOPO models tend to underestimate the surface area impounded for low reservoir water levels (true positive rates are low), even though the impounded surface extracted from them remains within the limits of the real impounded surface for a given reservoir water level (precision is high). In opposition, SfM models tend to overestimate the surface area impounded for low reservoir water levels (precision is low), although the limits of the real impounded surface are well comprised within the limits of the impounded surface estimated from them (true positive rates are high). Irrespective of decreasing reliability with lowering

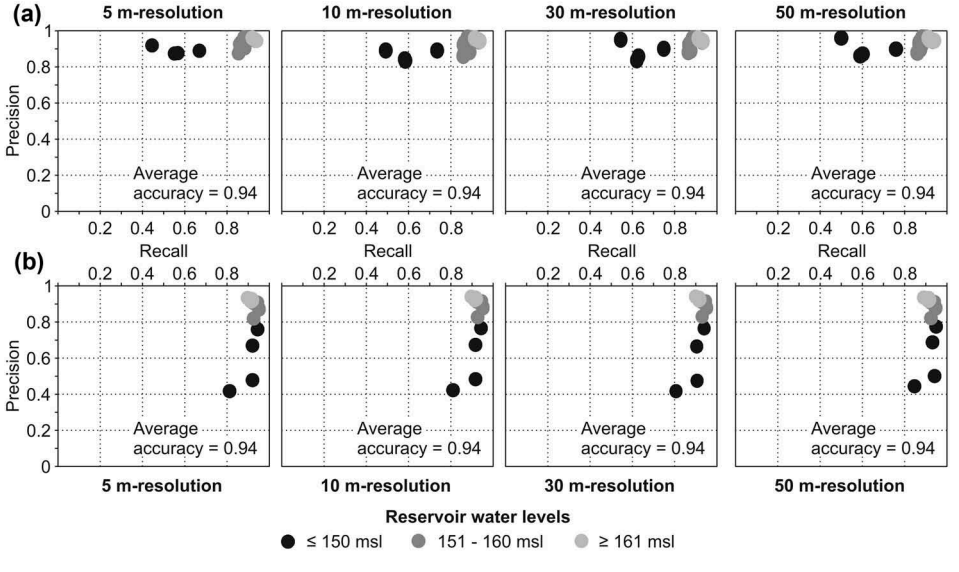

Figure 9. Precision-recall curves for (a) TOPO models and (b) SfM models by sampling resolution.

reservoir water levels (or increasing reservoir depth), average accuracy indicates that both TOPO and SfM DEMs perform fine for all sampling resolutions.

Discussion

Reconstructing the bathymetry of aged reservoirs is inherently complex because elevation data sources decrease in availability and reliability with time backwards. In addition, the time and the cost inherent to conducting bathymetric surveys make this kind of information unavailable or discontinuous for many regions worldwide. Topographic data prior to dam closure remain essential because they reveal terrain forms that provide crucial insights for reservoir storage capacity management and projection through area-volume-elevation curves (Cross and Moore 2014, Sayl *et al*. 2017). Furthermore, the understanding gained from sedimentation models run on the basis of accurate and reliable parameters of the reservoir geometry is essential for predicting the future response of reservoirs to population and climate changes (Watts *et al*. 2011, Kondolf *et al*. 2014, Ehsani *et al*. 2017).

This paper tested and compared the accuracy and the reliability of TOPO- and SfM-derived DEMs of varying resolution to reconstruct the topography of an average-aged reservoir prior to dam closure. Although all DEMs were of acceptable quality, there were slight quality disagreements between primary model types and sampling resolutions. TOPO DEMs emerged as the most accurate models in terms of vertical fit; i.e. they showed the lowest RMSE, and a low proportion of outliers with the lowest magnitude. On the other hand, SfM DEMs emerged as the most accurate models in terms of elevation variety; i.e. they provided the greatest topographic detail. However, different interpolation techniques produced different types of error, which increased (or decreased) with increasing (or decreasing) resolution as a function of their nature, and relative to the terrain complexity. Errors in contour-derived DEMs result from deficiencies of the interpolation algorithm relative to the relationship between the density of contours used in interpolation and the complexity of the terrain surface (Wise 2000, Hengl *et al*. 2004, Fisher and Tate 2006). TOPO DEMs were affected by this relationship in various ways. First, elevation errors were linked to the contour spacing relative to terrain characteristics Since heights between contours are not necessarily equally distributed – such as it is assumed by the interpolating algorithm – errors in flatlands may be as large as the contour interval (Carrara *et al*. 1997), and will tend to decrease with increasing terrain energy unless slopes are too steep (Hengl *et al*. 2004), or are heavily dissected by steeped terrain forms (Wise 2000). Second, elevation errors increased with increasing grid cell size, and revealed a clear tendency to lowering elevation with resolution irrespective of the terrain characteristics. Vertical accuracy loss with lowering resolution has been reported elsewhere (Gao 1997, Pardo Pascual *et al*. 2002, Ziadat 2007), and results from a systematic attenuation of the relief as the DEM resolution becomes coarser (Grohmann 2015). Third, TOPO DEMs were affected by artefacts, with a clear dominance of flatland terracing and outlier clustering in rolling lands. Artefacts result from limitations of the interpolation algorithm relative to the contour spacing and shape (Hengl *et al*. 2004), and their distribution on a DEM was therefore found to be spatially correlated to terrain forms (Bonin and Rousseaux 2005, Carlisle 2005, Erdoğan 2010). Interestingly, artefacts were found to behave differently with increasing grid cell size.

Whereas elevation variety improved notably, outliers increased in proportion and magnitude. These trends may be explained using the approach of Xie *et al*. (2003). Flatlands are represented by single-value cells or SVC (i.e. cells defined by one single contour) and by no-value cells or NVC (i.e. cells estimated by interpolation of nearby SVC). As the grid resolution increases, elevation variety increases as well because NVCs and SVCs are progressively integrated into multi-value cells or MVC. In areas of steep slope, however, interpolation from two or more contour lines fails to address elevation in large MVCs, and so local outliers increase along with grid cell size.

Errors in photogrammetry-derived models may involve a variety of sources including camera internal parameters, imaging settings, and processing algorithms and software (Dai *et al*. 2014). Although SfM restitution solves the camera pose and scene geometry simultaneously and automatically (Westoby *et al*. 2012), SfM works by matching image texture in different photographs as in traditional photogrammetry (James and Robson 2012, Fonstad *et al*. 2013, Micheletti *et al*. 2015b). It therefore follows that SfM-derived DEMs will reflect intrinsic image texture-related limitations. For example, areas showing little texture or different coloration at different orientations will yield poor point clouds and may not be reconstructed (James and Robson 2012, Fonstad *et al*. 2013), and locations occluded from multiple viewing such as areas masked by vegetation or shadows may lead to incomplete point cloud coverage as well (Dandois and Ellis 2013, Micheletti *et al*. 2015a). Texture-related changes in multiple viewing images may explain a good proportion of artefacts within SfM DEMs presented herein. Although dense vegetation and artificial structures are absent, our study area exhibits alternating crop, grazing and fallow fields that may induce local variations of the ground level in flatlands, and is dissected by steeped terrain forms (valleys and hills) that may affect restitution results in rolling lands due to the effects of shading. Artefacts will therefore cluster in noisy areas where reflectance or topographic effects difficult detection of key points and tie point matching (Mölg and Bolch 2017). Furthermore, the quality of DEMs derived from dense point clouds will be additionally affected by the efficiency of the interpolating algorithm relative to the point density. Unfortunately, PhotoScan provides too little information on the interpolation technique it uses to create DEMs. It is mentioned, however, that DEMs are built using Inverse Distance Weighting (IDW) interpolation. In this case, IDW could be responsible for a good proportion of error in flat areas because of the low point density on which to base an accurate interpolation. Despite these limitations, SfM DEMs were of high relative quality, and elevation errors remained within the error range reported for other SfM-derived DEMs (e.g. −6.6 to 10.5 m SfM-LIDAR difference in Pedernales River; Fonstad *et al*. 2013, 4.9 m RMSE in Zmuttgletscher glacier; Mertes *et al*. 2017, 4.4 m RMSE in Ny Ålesund glacier; Mölg and Bolch 2017).

On the other hand, reliability analysis revealed that all eight DEMs were highly consistent to reproduce area–elevation relationships irrespective of the primary model type and resolution. This was particularly true for medium and high reservoir water levels; as for the lowest reservoir water levels (or the highest reservoir depths), TOPO DEMs were comparatively less sensitive (i.e. area–elevation relationships were underestimated), and SfM DEMs were comparatively less precise (i.e. area–elevation relationships were overestimated). These results indicate the effects of complex topography on the bottom of the reservoir lake. Indeed, the river flowed confined within a broad, deeply incised valley flanked by steeped terrace levels. It is therefore not surprising that DEMs are less reliable to reconstruct area–elevation relationships within such a contrasting topographic setting. Yet different processing methods

produce different types of error: (i) TOPO DEMs underestimate area–elevation relationships because the interpolation algorithm fails to estimate altitudes within semi-closed contours representing a roughly flat valley floor (Wise 2000); (ii) SfM DEMs overestimate altitudes due to the fattening effect induced by complex terrain against the uniform motion assumption (Jalobeanu 2011). Irrespective of the direction of error, low reliability in low-level area-elevation estimations will logically propagate into storage capacity predictions, and will have a direct impact on computations of capacity loss because they affect the zone allocated to the dead volume; i.e. the reservoir zone where sedimentation occurs. Thus, volume calculations derived from the DEMs produced herein should be conducted carefully, as DEMs must be corrected prior to computing AVE-based estimates and derivatives.

Which model to choose then?

Results from this investigation revealed that there is no clear superiority of one processing method to reproduce accurate and reliable terrain elevation and forms. One major advantage of new SfM photogrammetry over traditional contour line interpolation is that it allows reconstructing topography with acceptable quality and fine resolution for large-scale areas in few hours. In addition, using SfM with aerial topography brings new and interesting possibilities for environmental analysis through diachronic applications (Derrien *et al*. 2015, Gomez *et al*. 2015, Mertes *et al*. 2017, Mölg and Bolch 2017, Warrick *et al*. 2017). From a hydrological point of view, SfM models may have several additional benefits over traditional contour-derived DEMs. First, the relative accuracy of SfM DEMs was markedly superior and, in DEM-based hydrological analysis, accuracy in the representation of terrain forms is notably more important than accuracy in terrain elevation (Kenward *et al*. 2000, Wise 2000). Second, SfM models provided detailed information on microforms that may be very useful to compute sedimentation rates because they allow detecting zones that promote or prevent sedimentation. Yet SfM models are markedly affected by image texture homogeneity and/or change from multiple viewing (James and Robson 2012, Fonstad *et al*. 2013). Furthermore, there is still a number of questions to solve regarding the use of aerial photography as input for SfM models, especially regarding intrinsic image resolution, quality, geometry and overlapping issues (Gomez *et al*. 2015). As for the choice of a given model resolution, previous experience has demonstrated that coarser resolutions are more suitable for hydrological modelling (Wang *et al*. 2000, Le Coz *et al*. 2009, Nourani *et al*. 2013), whilst hillslope and other hydrologically significant terrain details can be lost (Hancock 2005, Grohmann 2015). We therefore suggest restricting the use of fine DEM resolutions (<10m) for analysis requiring high topographic detail, such as computation of sedimentation rates, as coarser DEM resolutions have little influence on large-scale hydrologic predictions and contribute to accelerate the time required for processing notably.

Conclusions

This paper tested the applicability of two robust and widely applicable techniques – traditional contour line interpolation and new Structure-from-Motion photogrammetry – to obtain topographic data allowing reconstructing the bathymetry of average-aged reservoirs prior

to dam closure. Results outlined that both techniques hold great potential to reconstruct past topography with low money and time investments, and require a low level of expertise. Yet they both present intrinsic limitations, and the DEMs derived from them must be corrected to improve their hydrological plausibility. The greatest advantage of contour line interpolation over SfM photogrammetry is that intrinsic errors are well-known, and advances in computing and GISciences allow improving the quality of contour-derived DEMs notably. Indeed, SfM is a new automated technique developed to work intelligently with recent photography, and there is still a number of questions to solve relative to its performance with historic aerial photography and inherent resolution, quality, geometry and overlapping issues. Yet SfM DEMs provide the greatest variety of terrain landforms with high topographic detail, all of which opens an array of possibilities for environmental monitoring, prediction and management. It is therefore concluded that, for areas with similar terrain complexity, the implementation of one or another technique will depend ultimately on the users' need for preserving accurate elevation (contour interpolation) or topographic detail (SfM). In areas strongly vegetalized and/or exhibiting great terrain complexity, however, traditional contour-derived DEMs are expected to be more performant than new SfM DEMs for similar processing-related time cost and expertise.

Acknowledgments

The authors thank Dr Franck Vautier for providing assistance and constructive comments to the manuscript. This paper would not have the present form without the valuable comments and suggestions of Dr Sytze de Bruin and three anonymous reviewers.

Disclosure statement

No potential conflict of interest was reported by the authors.

Funding

Funding was provided to Ana Casado by the Consejo Nacional de Investigaciones Científicas y Técnicas (CONICET) post-graduate scholarship.

Notes on contributors

Ana Casado is a Research Fellow in the Departamento de Geografía y Turismo at the Universidad Nacional del Sur (Argentina). She also serves as Associate Member in the Laboratoire de Géographie Physique et Environnementale UMR 6042 GEOLAB at the Université Blaise Pascal (France), where she received her Ph.D. in Geography in 2013. Her research interests span hydrology and morphology of regulated rivers, climate variability & hydroclimatic extremes, and geosciences including GIS and 3D analysis & surface modelling.

Borbála Hortobagyi is a Research Associate in the School of Geography, Politics and Sociology at Newcastle University (UK). She also serves as Associate Member in the Laboratoire de Géographie Physique et Environnementale UMR 6042 GEOLAB at the Université Blaise Pascal (France), where she received her Ph.D. in Geography in 2018. Her research interests span fluvial geomorphology, biogeomorphology, river flow monitoring, and geosciences including GIS and 3D analysis & surface modelling.

Erwan Roussel is a Research Engineer in the Laboratoire de Géographie Physique et Environnementale UMR 6042 GEOLAB at the Université Blaise Pascal (France), where he received his Ph.D. in Geography in 2011. His research interests span glacial and fluvial adjustments to climate change, complex response of geomorphological systems, stone decay & cultural heritage, and geosciences including GIS, 3D analysis & surface modelling and geostatistics.

ORCID

Ana Casado http://orcid.org/0000-0003-4480-3756

References

Annandale, G., 2013. *Quenching the thirst: sustainable water supply and climate change*. North Charlesto, SC: CreateSpace Independent Publishing Platform.

Bohn, V.Y., Piccolo, M.C., and Perillo, G.M.E., 2011. Análisis de los periodos secos y húmedos en el sudoeste de la provincia de Buenos Aires (Argentina). *Revista De Climatología*, 11, 31–43.

Bonin, O. and Rousseaux, F., 2005. Digital terrain model computation from contour lines: how to derive quality information from artifact analysis. *GeoInformatica*, 9 (3), 253–268. doi:10.1007/s10707-005-1284-2

Campo, A.M., Ramos, M.B., and Zapperi, P., 2009. Análisis de las variaciones anuales de precipitación en el Suroeste bonaerense, Argentina. *In*: *XII Encuentro de Geógrafos de América Latina*, 3–7 April 2009 Montevideo, Uruguay, 12.

Carlisle, B.H., 2005. Modelling the spatial distribution of DEM error. *Transactions in GIS*, 9 (4), 521–540. doi:10.1111/tgis.2005.9.issue-4

Carrara, A., Bitelli, G., and Carla, R., 1997. Comparison of techniques for generating digital terrain models from contour lines. *International Journal of Geographical Information Science*, 11 (5), 451–473. doi:10.1080/136588197242257

Carrivick, J.L., Smith, M.W., and Quincey, D.J., 2016. *Structure from motion in the geosciences*. Chichester: John Wiley & Sons.

Ceylan, A. and Ekizoglu, I., 2014. Assesment of bathymetric maps via GIS for water in reservoir. *Boletim de Ciências Geodésicas*, 20 (1), 142–158. doi:10.1590/s1982-21702014000100010

Cross, B.K. and Moore, B.C., 2014. Lake and reservoir volume: hydroacoustic survey resolution and accuracy. *Lake and Reservoir Management*, 30 (4), 405–411. doi:10.1080/10402381.2014.960115

Dai, F., Feng, Y., and Hough, R., 2014. Photogrammetric error sources and impacts on modeling and surveying in construction engineering applications. *Visualization in Engineering*, 2 (2), 1–14. doi:10.1186/2213-7459-2-2

Dandois, J.P. and Ellis, E.C., 2013. High spatial resolution three-dimensional mapping of vegetation spectral dynamics using computer vision. *Remote Sensing of Environment*, 136, 259–276. doi:10.1016/j.rse.2013.04.005

Derrien, A., *et al*., 2015. Retrieving 65 years of volcano summit deformation from multitemporal structure from motion: the case of Piton de la Fournaise (La Réunion Island). *Geophysical Research Letters*, 42 (17), 6959–6966. doi:10.1002/2015GL064820

Desmet, P., 1997. Effects of interpolation errors on the analysis of DEMs. *Earth Surface Processes and Landforms*, 22 (6), 563–580. doi:10.1002/(ISSN)1096-9837

Ehsani, N., *et al*., 2017. Reservoir operations under climate change: storage capacity options to mitigate risk. *Journal of Hydrology*, 555, 435–446. doi:10.1016/j.jhydrol.2017.09.008

Erdoğan, S., 2010. Modelling the spatial distribution of DEM error with geographically weighted regression: an experimental study. *Computers & Geosciences*, 36 (1), 34–43. doi:10.1016/j.cageo.2009.06.005

Fawcett, T., 2006. An introduction to ROC analysis. *Pattern Recognition Letters*, 27, 861–874. doi:10.1016/j.patrec.2005.10.010

Felicísimo, A.M., 1994. Parametric statistical method for error detection in digital elevation models. *ISPRS Journal of Photogrammetry and Remote Sensing*, 49 (4), 29–33. doi:10.1016/0924-2716(94)90044-2

Fisher, P.F. and Tate, N.J., 2006. Causes and consequences of error in digital elevation models. *Progress in Physical Geography*, 30, 467–489. doi:10.1191/0309133306pp492ra

Fonstad, M.A., *et al*., 2013. Topographic structure from motion: a new development in photogrammetric measurement. *Earth Surface Processes and Landforms*, 38, 421–430. doi:10.1002/esp.3366

Frazier, P.S. and Page, K.J., 2000. Water body detection and delineation with landsat TM data. *Photogrammetric Engineering and Remote Sensing*, 66 (12), 1461–1468.

Gao, J., 1997. Resolution and accuracy of terrain representation by grid DEMs at a micro-scale. *International Journal of Geographical Information Sciences*, 11 (2), 199–212. doi:10.1080/136588197242464

Gomez, C., Hayakawa, Y., and Obanawa, H., 2015. A study of Japanese landscapes using structure from motion derived DSMs and DEMs based on historical aerial photographs: new opportunities for vegetation monitoring and diachronic geomorphology. *Geomorphology*, 1, 11–20. doi:10.1016/j.geomorph.2015.02.021

Grohmann, C.H., 2015. Effects of spatial resolution on slope and aspect derivation for regional-scale analysis. *Computers & Geosciences*, 77, 111–117. doi:10.1016/j.cageo.2015.02.003

Hancock, G.R., 2005. The use of digital elevation models in the identification and characterization of catchments over different grid scales. *Hydrological Processes*, 19, 1727–1749. doi:10.1002/(ISSN)1099-1085

Hengl, T., Gruber, S., and Shrestha, D., 2004. Reduction of errors in digital terrain parameters used in soil-landscape modelling. *International Journal of Applied Earth Observation*, 5, 97–112. doi:10.1016/j.jag.2004.01.006

Ho, M., *et al*., 2017. The future role of dams in the United States of America. *Water Resources Research*, 53 (2), 982–998. doi:10.1002/2016WR019905

Hutchinson, M.F., 1988. Calculation of hydrologically sound digital elevation models. *In*: *Third International Symposium on Spatial Data Handling*, 17–19 August 1988 Sidney, Australia. Columbus, Ohio: International Geographical Union, 117–133.

Hutchinson, M.F., 1989. A new procedure for gridding elevation and stream line data with automatic removal of spurious pits. *Journal of Hydrology*, 106, 211–232. doi:10.1016/0022-1694(89)90073-5

Jalobeanu, A., 2011. Predicting spatial uncertainties in stereo photogrammetry: achievements and intrinsic limitations. *In*: *7th International Symposium on Spatial Data Quality*, 12–14 October 2011 Coimbra, Portugal, 6.

James, M. and Robson, S., 2012. Straightforward reconstruction of 3D surfaces and topography with a camera: accuracy and geoscience application. *Journal of Geophysical Research: Earth Surface*, 117 (F3), 1–17. doi:10.1029/2011JF002289

Kang, B., *et al*., 2007. A flood risk projection for Yongdam dam against future climate change. *Journal of Hydro-Environment Research*, 1 (2), 118–125. doi:10.1016/j.jher.2007.07.003

Kenward, T., *et al*., 2000. Effects of digital elevation model accuracy on hydrologic predictions. *Remote Sensing & Environment*, 74, 432–444. doi:10.1016/S0034-4257(00)00136-X

Kim, S., *et al*., 2009. Reconsideration of reservoir operations under climate change: case study with Yagisawa Dam, Japan. *Annual Journal of Hydraulic Engineering, JSCE*, 53, 597–611.

Kondolf, G.M., *et al*., 2014. Sustainable sediment management in reservoirs and regulated rivers: experiences from five continents. *Earth's Future,* 2, 256–280. doi:10.1002/2013EF000184

Le Coz, M., *et al*., 2009. Assessment of Digital Elevation Model (DEM) aggregation methods for hydrological modeling: lake Chad basin, Africa. *Computers & Geosciences*, 35, 1661–1670. doi:10.1016/j.cageo.2008.07.009

Mertes, J.R., *et al*., 2017. Using structure from motion to create glacier DEMs and orthoimagery from historical terrestrial and oblique aerial imagery. *Earth Surface Processes and Landforms*, 42 (14), 2350–2364. doi:10.1002/esp.4188

Micheletti, N., Chandler, J.H., and Lane, S.N., 2015a. Investigating the geomorphological potential of freely available and accessible structure-from-motion photogrammetry using a smartphone. *Earth Surface Processes and Landforms*, 40 (4), 473–486. doi:10.1002/esp.3648

Micheletti, N., Chandler, J.H., and Lane, S.N., 2015b. Structure from motion (SfM) photogrammetry. *In*: L.E. Clarke and J.M. Nield, eds. *Geomorphological techniques (Online edition)*. London: British Society for Geomorphology.

Mölg, N. and Bolch, T., 2017. Structure-from-Motion using historical aerial images to analyse changes in glacier surface elevation. *Remote Sensing*, 9 (10), 1021–1038. doi:10.3390/rs9101021

Nourani, V., *et al*. 2013. Effect of DEM type and resolution in extraction of hydro-geomorphologic parameters. *In*: V. Mladenov, eds. *Recent advances in continuum mechanics, hydrology and ecology*. Rhodes Island, Greece: WSEAS, 98–103.

Pardo Pascual, J.E., Acosta Matarredona, P., and Porres de la Haza, M.J., 2002. Quality assesment of digital elevation models deduced from digital cartography for hydrogeomorphological applications. *In*: *3ª Asamblea Hispano Portuguesa de Geodesia y Geofísica*, 4–8 February 2002 Valencia, Spain, 1746–1750.

Saito, T. and Rehmsmeier, M., 2015. The precision-recall plot is more informative than the ROC plot when evaluating binary classifiers on imbalanced datasets. *PloS One*, 10 (3), e0118432. doi:10.1371/journal.pone.0118432

Sayl, K.N., Muhammad, N.S., and El-Shafie, A., 2017. Optimization of area–volume–elevation curve using GIS–SRTM method for rainwater harvesting in arid areas. *Environmental Earth Sciences*, 76 (10), 368. doi:10.1007/s12665-017-6699-1

Schefer, J.C., 2004. *Los recursos hídricos y el abastecimiento de agua*. Bahía Blanca: CEPADE.

Scian, B., 2000. Episodios ENSO y su relación con las anomalías de precipitación en la pradera pampeana. *Geoacta*, 25, 23–40.

Soundharajan, B.-S., Adeloye, A.J., and Remesan, R., 2016. Evaluating the variability in surface water reservoir planning characteristics during climate change impacts assessment. *Journal of Hydrology*, 538, 625–639. doi:10.1016/j.jhydrol.2016.04.051

Wang, M., Hjelmfelt, A.T., and Garbrecht, J., 2000. DEM aggregation for watershed modeling. *Journal of the American Water Resources Association*, 36, 579–584. doi:10.1111/jawr.2000.36.issue-3

Warrick, J.A., *et al*., 2017. New techniques to measure cliff change from historical oblique aerial photographs and structure-from-motion photogrammetry. *Journal of Coastal Research*, 33 (1), 39–55. doi:10.2112/JCOASTRES-D-16-00095.1

Watts, R.J., *et al*., 2011. Dam reoperation in an era of climate change. *Marine and Freshwater Research*, 62 (3), 321–327. doi:10.1071/MF10047

WCD, 2000. *Dams and development. A new framework for decision-making*. London: Earthscan Publications.

Westoby, M.J., *et al*., 2012. 'Structure-from-Motion' photogrammetry: A low-cost, effective tool for geoscience applications. *Geomorphology*, 179, 300–314. doi:10.1016/j.geomorph.2012.08.021

Wise, S.M., 2000. Assessing the quality for hydrological applications of digital elevations models derived from contours. *Hydrological Processes*, 14, 1909–1929. doi:10.1002/1099-1085(20000815/30)14:11/12<1909::AID-HYP45>3.0.CO;2-6

Xie, K., *et al*., 2003. Using contour lines to generate digital elevation models for steep slope areas: a case study of the Loess Plateau in North China. *Catena*, 54, 161–171. doi:10.1016/S0341-8162(03)00063-8

Ziadat, F.M., 2007. Effect of contour intervals and grid cell size on the accuracy of DEMs and slope derivatives. *Transactions in GIS*, 11 (1), 67–81. doi:10.1111/tgis.2007.11.issue-1